

# **Design Optimization and Performance of Pumping Options for VTR Extended Length Test Assembly for Lead Coolant (ELTA-CL) - Update**

Mohamed S. El-Genk, Timothy Schriener, Ragai  
Altamini and Andrew Hahn

*Institute for Space and Nuclear Power Studies and Nuclear Engineering  
Department, University of New Mexico, Albuquerque, NM, 87131*

**Technical Report Number: UNM-ISNPS-5-2020**  
Performance Period: June 2020 – September 2020

Work funded by Battelle Energy Alliance, LLC,  
Award No. 145662 to the University of New Mexico.

September 30, 2020

## Executive Summary

The University of New Mexico’s Institute for Space and Nuclear Power Studies (UNM-ISNPS) has been tasked with conducting design optimization and performance and Computational Fluid Dynamics (CFD) of four pumping options for the Los Alamos National Laboratory’s (LANL) Extended Length Test Assembly for Lead Coolant (ELTA-CL) for the Versatile Test Reactor (VTR) currently being developed under the direction of the US Department of Energy, Office of Nuclear Energy. This report updates the information provided in an earlier technical issued by UNM-ISNPS in June 2020 (El-Genk et al., 2020), detailing the progress made in the period from June to September 2020. The following tasks are accomplished during that period:

- (a) An integrated thermal-hydraulic model of the ELTA-CL is developed to estimate the demand curves for different designs, the reference LANL design with a riser tube diameter of 57.0 mm and two other designs by LANL and UNM-ISNPS with a riser tube diameter of 68.8 mm but different lead downcomer widths. The intersections of the calculated demand curves of the different ELTA-CL designs with the obtained supply curves for the different pumping options determine the expected pumping head and circulation flow rate of the molten lead, as well as the average flow velocities in three different 3-rod bundle geometries, one with a circular shroud, and two with scalloped shrouds and increasingly reduced flow areas. The locations and the values of the corresponding maximum flow velocities in the bundle geometries are determined using 3-D, CFD analysis, for same fuel rod diameter and pitch.
- (b) The developed ELTA-CL thermal-hydraulics model is used to investigate the heat rejection capabilities of the three different ELTA-CL designs to the VTR sodium coolant and the effects of the pumping option, the test bundle geometry, and the width of the He gap in the wall separating the molten lead downcomer from the VTR flow, on the average linear power of the fuel rods in the three different 3-rod test bundles.
- (c) Improved the design of the four pumping options investigated for the ELTA-CL are detailed in UNM-ISNP June report (El-Genk et al., 2020). These options are:
  - (1) Gas Lift Pumping (GLP),
  - (2) miniature submerged Annular Linear Induction Pump (ALIP),
  - (3) miniature submerged DC Electromagnetic Pump (DC-EMP), and
  - (4) miniature axial-centrifugal flow Mechanical Pump (MP).
- (d) Contrasted the performance results of the latest improved designs of these pumping options to the desired testing capabilities and requirements for ELTA-CL (Table 1). These include the average and maximum flow velocities in 3-rod test bundles of the different geometries and the rod average linear power for the planned Phase 1 testing. All design and performance analyses are done for a Pb exit temperature of 500°C.

**Table 1:** Desired ELTA-CL Capabilities / Requirements

Parameter	Value/Range
<b>Rod Peak / Average (*) Linear Power (W/cm)</b>	<b>400 / 250 (steady state), *assume axial Cosine</b>
<b>Average Lead Velocity in Test Bundles (m/s)</b>	<b>Up to at least 3.0</b>
<b>Max. / Min. Lead temperature (°C)</b>	<b>Up to 550 in Phase 1 and 750 in Phase 2 / 400</b>

## Table of Contents

Executive Summary	2
List of Figures	3
List of Tables	4
1. ELTA-CL Design Options Investigated	5
1.1. <i>ELTA-CL Demand Curves</i>	7
1.2. <i>ELTA-CL Heat Rejection and Test Rod Average Linear Power</i>	7
2. The Gas Lift Pumping (GLP) Option for ELTA-CL	8
2.1 <i>Performance of GLP for ELTA-CL with 3m Tall Riser</i>	9
2.2. <i>Effect of Riser Length on Performance of GLP Option</i>	10
3. Improved Designs of the Annular Linear Induction Pump (ALIP)	11
3.1. <i>Effects of ALIP Length and Wire Diameter on Performance</i>	11
4. Improved Design of Direct Current-Electromagnetic Pump (DC-EMP)	14
4.1. <i>DC-EMP Performance Characteristics</i>	15
5. Improved Design of Axial Centrifugal Flow Mechanical Pump (MP)	17
5.1 <i>MP Performance Results</i>	17
6. Summary and Findings	20
References	22

## List of Figures

<b>Fig. 1:</b> Calculated velocity contours using 3D thermal-hydraulic analyses of molten lead flow in the 3-rod bundle geometries in Table 3, with and without scalloped shroud walls, at $T_{in} = 420^{\circ}\text{C}$ , $T_{ex} = 500^{\circ}\text{C}$ , and mass flow rate, $\dot{m} = 6 \text{ kg/s}$ .	6
<b>Fig. 2:</b> Comparison of calculated demand curves of ELTA-CL design options and different geometries of the 3-rod test bundles in present analyses for Pb exit temperature of $500^{\circ}\text{C}$ .	6
<b>Fig. 3:</b> Achievable test rods average linear powers for ELTA-CL at Pb $T_{ex} = 500$ and $700^{\circ}\text{C}$	7
<b>Fig. 4:</b> Comparison of GLP option performance curves at Pb exit temperature of $500^{\circ}\text{C}$ in ELTA-CL designs in Table 2, with 3 m long riser above the 3-rod test bundle	8
<b>Fig. 5:</b> Effect of riser length on Pb flow rate in the ELTA-CL LANL Option 1 design (Table 1) using GLP option at a Pb exit temperature, $T_{ex}$ , of $500^{\circ}\text{C}$	9

<b>Fig. 6:</b> Calculated ALIP performance characteristics at a molten lead exit temperature of 500°C	12
<b>Fig. 7:</b> Improved DC-EMP Design for ELTA-CL with riser tube diameters of 57.0 and 68.8 mm	14
<b>Fig. 8:</b> Calculated DC-EMP performance characteristics at a molten lead temperature of 500°C	15
<b>Fig. 9:</b> MP performance characteristics at a molten lead exit temperature of 500°C	18

### **List of Tables**

<b>Table 1:</b> Desired ELTA-CL Capabilities / Requirements	2
<b>Table 2:</b> Geometric parameters and dimensions of ELTA-CL designs investigated	5
<b>Table 3:</b> Geometric parameters and dimensions of 3-rod bundle test sections investigated	5
<b>Table 4:</b> Comparison of GLP performance for the three investigated ELTA-CL design options	10
<b>Table 5:</b> Comparison of the performance of the best performing ALIPs for ELTA-CL at 500°C	13
<b>Table 6:</b> Performance comparisons of the developed improved DC-EMPs for the three designs of the ELTA-CL in Table 2 at molten Pb temperature of 500°C	16
<b>Table 7:</b> Comparison of the performance parameters of the optimized MP designs for ELTA-CL at Pb temperature of 500°C	19
<b>Table 8:</b> Comparison summary of the performance of the four pumping options investigated for the ELTA-CL at molten Pb exit temperature of 500°C	20

## 1. ELTA-CL Design Options Investigated

The performed analyses included three different ELTA-CL designs with different riser tube diameters and molten lead downcomer widths (Table 2), namely:

1. The baseline LANL Option 1 design has a riser tube of a 2" schedule 5 pipe with an inner diameter of 57.0 mm, and a downcomer width of 12.56 mm.
2. The LANL Option 2 design, which has a larger 2.5" schedule 5 riser pipe with an inner diameter of 68.8 mm and a smaller downcomer width of 6.21 mm.
3. The UNM-ISNPS Option, with a downcomer width of 11.24 mm and riser tube inner diameter of 68.8 mm.

**Table 2:** Geometric parameters and dimensions of ELTA-CL designs investigated

Parameters	LANL Option 1	LANL Option 2	UNM-ISNPS Option
<b>Riser Pipe</b>	2" SCH 5	2.5" SCH 5	2.5" SCH 5
Inner Diameter, $D_{riser}$ (mm)	57.0	68.8	68.8
Wall Thickness (mm)	1.65	2.11	2.11
Downcomer Width, $\delta_{dc}$ (mm)	12.56	6.21	11.24
<b>Downcomer Pipe</b>	Machined 3.5" SCH 80	Machined 3.5" SCH 80	Machined 3.5" SCH 10
Inner Diameter (mm)	85.45	85.45	95.50
Wall Thickness (mm)	4.78	4.78	2.19
Gas Gap Width (mm)	1.19	1.19	1.19
<b>Outer Pipe</b>	3.5" SCH 5	3.5" SCH 5	Machined 4" SCH 10
Outer Diameter (mm)	101.6	101.6	106.5
Wall Thickness (mm)	2.11	2.11	2.11
Hexagonal duct flat-to-flat (mm)	117		
Hexagonal duct thickness (mm)	3		

In all three ELTA-CL designs in Table 2, the ALIP, EMP and MP designs and gas injection nozzle for the GLP option are placed in the riser tube above the 3-rod test article. The pressure-flow rate demand curves for the ELTA-CL (Table 2) are calculated for three geometries of the 3-rod fuel bundle, termed Circular, Scalloped A, and Scalloped B (Fig. 1 and Table 3).

**Table 3:** Geometric parameters and dimensions of 3-rod bundle test sections investigated.

Dimensions and Parameters	Circular shroud	Scalloped A shroud	Scalloped B shroud
Fuel Rod diameter, d (mm)	10.7	10.7	10.7
Pitch, P (mm)	13.3	13.3	13.3
Rod P/d ratio	1.243	1.243	1.243
Shroud outer diameter (mm)	33.34	33.34	33.34
Rod-shroud wall distance (mm)	3.64	3.64	1.80 (LANL)
Cross section flow area ( $\text{mm}^2$ )	603.1 (1.0)	385.1 (0.639)	207.8 (0.345)
Wetted perimeter (mm)	205.6	200.2	190.4
Eq. hydraulic diameter (mm)	11.74	7.69	4.37

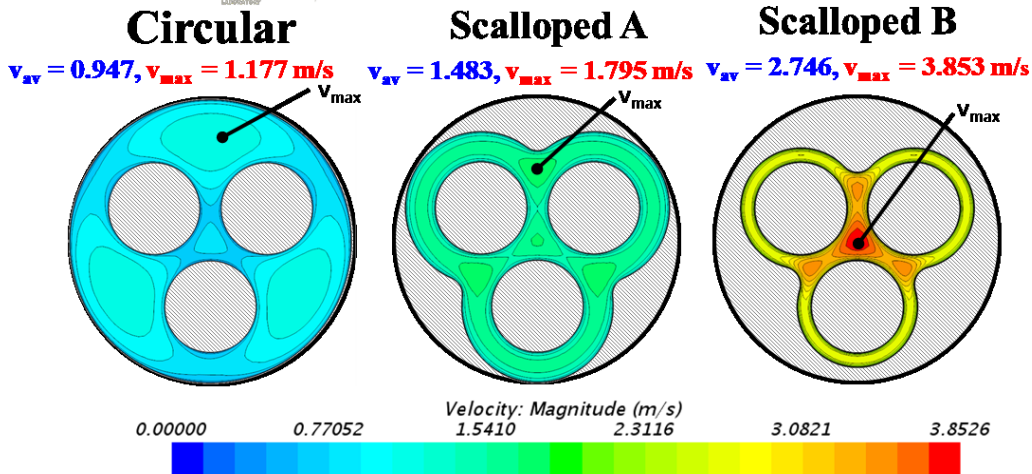


**Fig. 1:** Calculated velocity contours using 3D thermal-hydraulic analyses of molten lead flow in the 3-rod bundle geometries in Table 3, with and without scalloped shroud walls, at  $T_{in} = 420^{\circ}\text{C}$ ,  $T_{ex} = 500^{\circ}\text{C}$ , and mass flow rate,  $\dot{m} = 6 \text{ kg/s}$ .

Table 3 shows that the cross sectional flow area of the Scalloped A bundle geometry is 63.9% of that for the Circular geometry, while the cross section flow areas for the Scalloped B geometry is only 34.5% of that for the Circular bundle. The performed 3D CFD analyses investigated the effect of scalloping the shroud on the flow fields, the average velocity,  $v_{av}$ , and both the value and location of the maximum velocity,  $v_{max}$ , for the three different bundle geometries in Fig. 1, at the same total flow rate of 6 kg/s and molten lead velocity of  $500^{\circ}\text{C}$ .

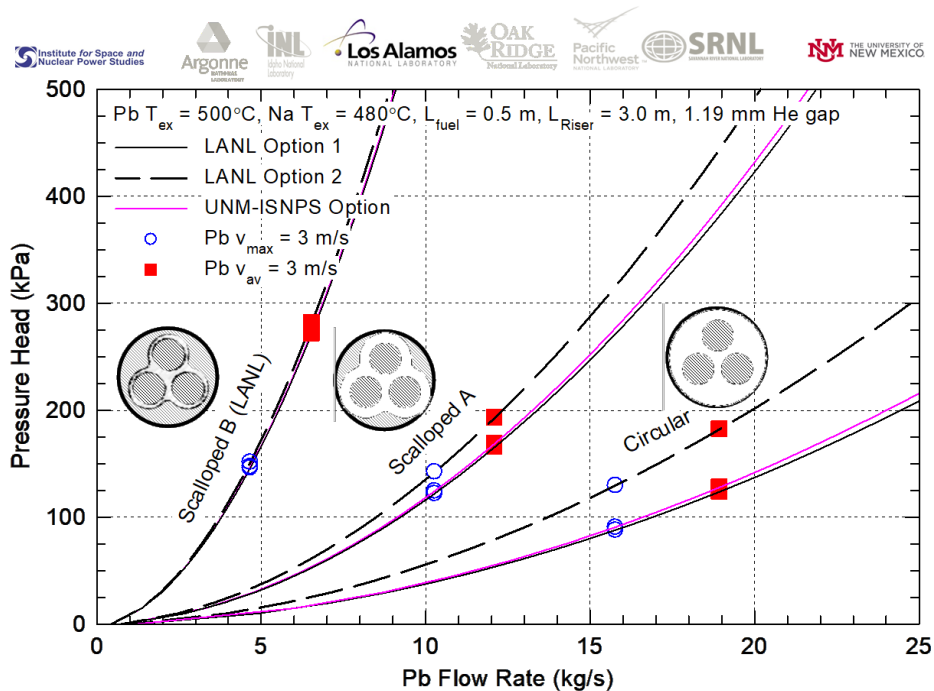


**Fig. 2:** Comparison of calculated demand curves of ELTA-CL design options and different geometries of the 3-rod test bundles in present analyses for Pb exit temperature of  $500^{\circ}\text{C}$ .

### 1.1. ELTA-CL Demand Curves

The calculated pressure head (or losses) - flow rate demand curves for the ELTA-CL designs detailed in Table 2 and with the different test rod bundle geometries in Table 3 are compared in Fig. 2. The developed ELTA-CL model also calculates the rate of heat removal from the flowing molten Pb flowing in the annular downcomer to the up flow the VTR Na coolant. They are separated by the double steel wall with a He gap, that is 1.19 mm wide for all three ELTA-CL designs investigated (Table 1). Fig. 2 indicates the combined values of the Pb flow rate and total pressure losses to achieve average and maximum flow velocities in the 3-rod test bundles of 3 m/s. The pressure-flow rate demand for the LANL Option 1 and UNM-ISNPS Option of the ELTA-CL design are nearly the same, as the widths of the annular downcomer are comparable (Table 1). The high-pressure losses in Scalloped B 3-rod test bundle (Fig. 1) make the effects of the riser diameter and the downcomer width on the total pressure losses insignificant (Fig. 2).

### 1.2. ELTA-CL Heat Rejection and Test Rod Average Linear Power

The average linear power for the test fuel rods in the ELTA-CL is practically limited by the rate of heat rejection to the VTR primary Na. Because of the low Peclet numbers for the molten lead flow in the downcomer of the ELTA-CL and the VTR primary sodium, the heat transfer coefficients for both are practically constant and independent of the circulation rate of molten Pb, and hence the pumping power option. Thus, the rate of heat rejection from the ELTA-CL to the VTR Na flow depends almost solely on the width of the He gap (Table 1) and the molten lead exit temperature.

The results presented in Fig. 3 show the effects of the He gap width and Pb exit temperature of the total heat rejection from the ELTA-CL and hence the attainable average linear power of the test fuel rods (with total length of 100.0 cm and an active length of 50.0 cm). With a 1.19 mm wide He gap, the desirable range of the average linear power could not be achieved, when operating with a Pb exit temperature of 500°C (Table 1). However, for this Pb temperature, and 0.5 mm wide He gap, the average linear power for the test rods would meet the ELTA-CL desirable requirements (Table 1). At the higher Pb exit temperature 700°C, and with the reference He gap width of 1.19 mm, the average linear powers for the test rod could far exceed the ELTA-CL desired requirements (Table 1).

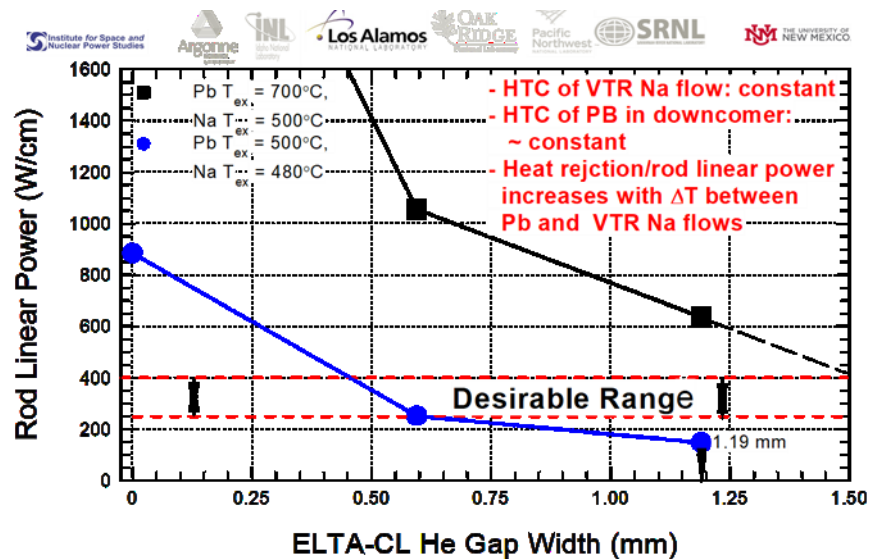
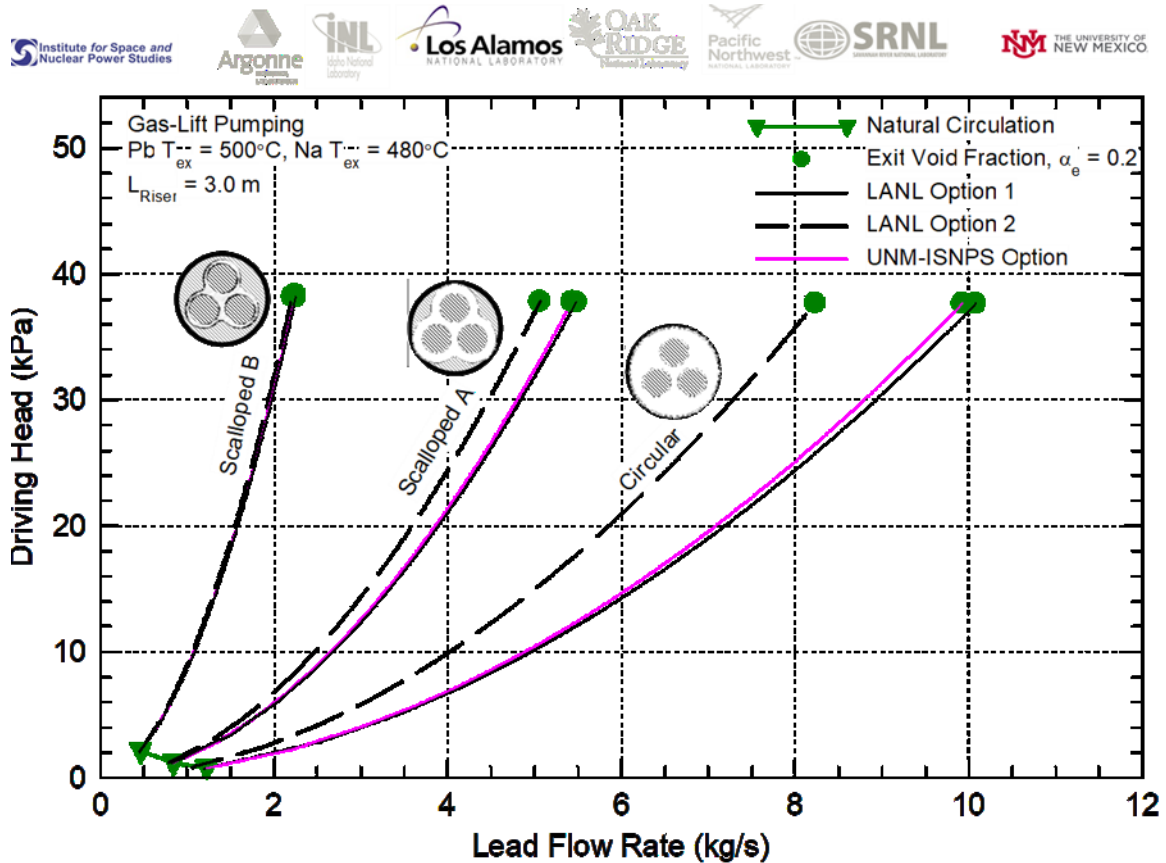


Fig. 3: Achievable test rods average linear powers for ELTA-CL at Pb T<sub>ex</sub> = 500 and 700°C.

## 2. The Gas Lift Pumping (GLP) Option for ELTA-CL

The Gas-Lift Pumping (GLP) option circulates the molten lead in the ELTA-CL by increasing the buoyant force for natural circulation. The injected gas bubbles in the riser tube above the test rod bundles decreases the average density in the riser, and hence, the weight of the liquid/gas mixture in the riser tube relative to that of the molten lead in the downcomer of the ELTA-CL. The resulting weight difference increases the circulation of the molten lead in the ELTA-CL. Effective operation of the gas lift option requires maintaining the gas-molten lead mixture in the riser in the bubbly flow regime. Otherwise, bubbles coalescence in the riser will shift the flow to the slug or the churn regimes, negatively impacting the circulating rate of molten lead and resulting in flow chugging in the riser.



**Fig. 4:** Comparison of GLP option performance curves at Pb exit temperature of 500°C in ELTA-CL designs in Table 2, with 3 m long riser above the 3-rod test bundle.

While in the bubbly flow regime, increasing the gas injection rate in the riser tube would enhance the circulation rate (Fig. 4). For the same exit void fraction for bubbly flow regime of up to 0.20, increasing the riser length up to 3.0 m effectively increases the molten lead circulation rate (Fig. 5), depending on the 3-rod test bundle geometry. Beyond such length, increasing the riser length decreases the average gas void fraction, only slightly increasing the circulation rate.

A two-phase flow map for heavy liquid metals-gas flows has developed for the bubbly to slug flow transition. Based on the reported experimental data of Shi et al. (2018) for Lead Bismuth Eutectic (LEB)-Ar flows and of Nishi et al. (2003) for LBE-N<sub>2</sub> flows the transition

between the bubbly and slug flow regimes has been found by UNM-ISNPS team to occur at an exit void fraction of 0.2 (El-Genk et al., 2020). Therefore, to ensure remaining in the bubbly flow region in the riser, the exit void fraction at the free surface of the molten lead in the ELTA-CL should not exceed 0.2.

The developed thermal hydraulics natural circulation model of the ELTA-CL, with and without the GLP option, in the Simulink/Matlab platform investigated the effects of the riser length and injection rate of the Argon gas into the riser on the developed driving pressure head and the corresponding circulation rate of molten Pb. This is at an exit temperature of 500°C and with different 3-rod bundles geometries in Table 2. The developed gas lift model for the ELTA-CL is successfully validated (El-Genk et al., 2020) using reported data from LBE-N<sub>2</sub> gas lift experimental loop of Nishi et al. (2003), and from the LBE-Ar gas lift experimental loop of Shi et al. (2018). The model predictions show good agreement with the trend of the reported data for both experiments. The validated model investigated the effects on enhancing the GLP performance for ELTA-CL of: (1) increasing the riser tube diameter (57.0 and 68.8 mm), (2) increasing the riser height up to 8 m above the test rod bundles, and (3) increasing the Pb exit temperature (500 °C and 700°C)

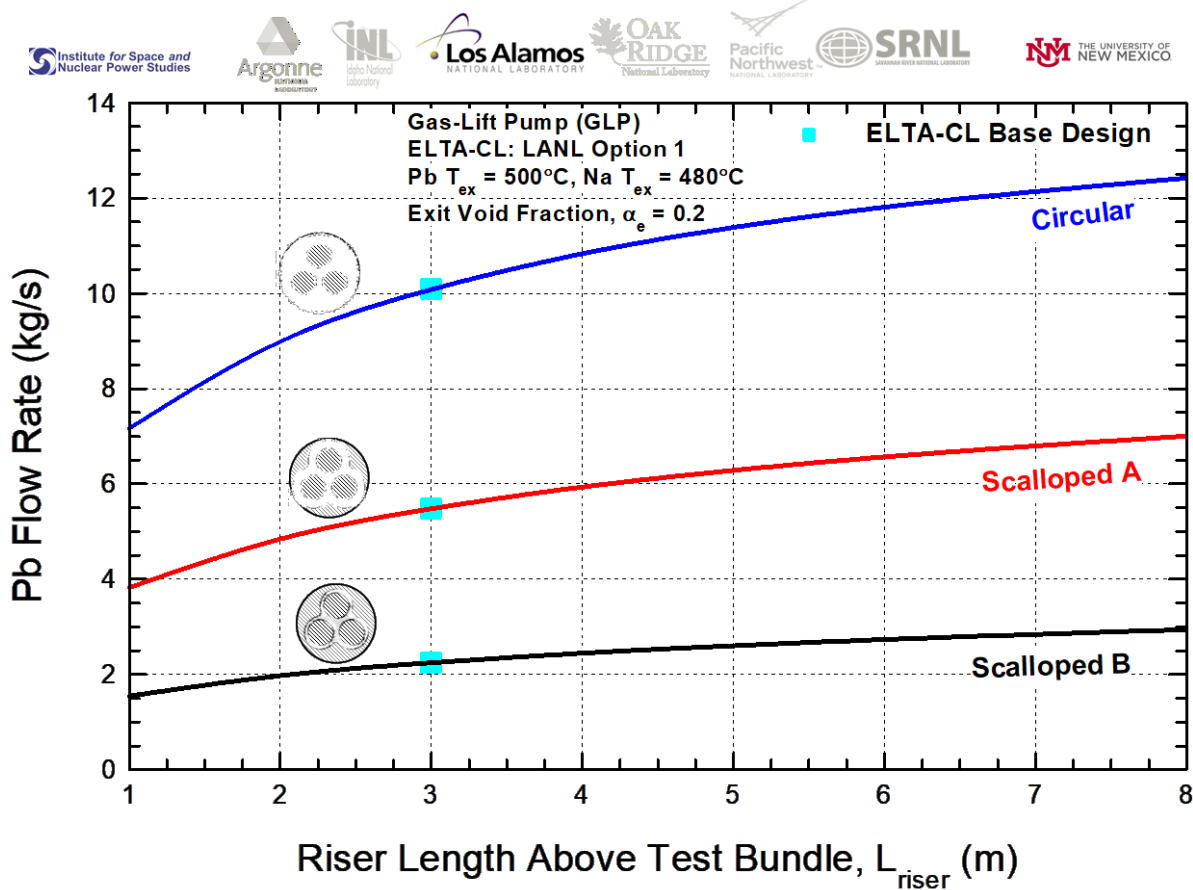


**Fig. 5:** Effect of riser length on Pb flow rate in the ELTA-CL LANL Option 1 design (Table 1) using GLP option at a Pb exit temperature, T<sub>ex</sub>, of 500°C.

### 2.1 Performance of GLP for ELTA-CL with 3m Tall Riser

Figure 4 shows the calculated driving head and flow rate for the three different ELTA-CL design options in Table 2, with 3 m tall riser, using the present GLP option. For all ELTA-CL

design options, the achievable driving pressure heads at an exit void fraction of 0.2 range from ~37 to 38 kPa. The GLP performance curves for the LANL ELTA-CL design Option 1 and the proposed UNM-ISNPS design are almost identical, while those for the LANL design Option 2 are higher (Fig. 4). The lower bounds of these curves are the values corresponding to Pb liquid natural conversion with zero gas injection in the ELTA-CL riser (indicated by the solid triangle symbols in Fig. 4).

With the 3-m long riser tube, natural circulation can achieve only a low flow velocity in the 3-rod test bundles of ~ 0.2 m/s. For the same molten Pb exit temperature of 500°C, the flow velocity would increase with increasing the riser length. However, increasing the molten lead exit temperature to 700°C would also enhance natural circulation in the ELTA-CL and the average flow velocity in the test rod bundles.

The GLP performance results in Fig. 4 show that increasing the Ar injection rate in the riser until reaching an exit void fraction,  $\alpha_e$ , of 0.2 increases the average flow velocity of molten lead in the different 3-rod test bundle geometries (Fig. 1) up to 1.60 m/s (Table 4). This is well below the desired 3 m/s for ELTA-CL (Table 1). Increasing the riser diameter from 57.0 mm for the LANL Option 1 design to ELTA-LC to 68.8 mm for the UNM-ISNPS design option results in nearly the same flow rate, but increases the Ar gas injection rate for  $\alpha_e = 0.2$  by 20-30%. Table 4 compared the GLP option for the three ELTA-CL designs investigated in this work with a riser height of 3 m and molten lead exit temperature of 500°C.

**Table 4:** Comparison of GLP performance for the three investigated ELTA-CL design options.

Bundle Geometry	Head / Pb Flow (kPa / kg/s)	Injected Ar Gas (mg/s)	Compliance with ELTA-CL Requirements				
			Velocity (m/s)		Met?	Linear Power (W/cm)	Met?
			V <sub>av</sub>	V <sub>max</sub>			
<b>ELTA-CL LANL Option 1: <math>L_{\text{riser}} = 3 \text{ m}</math>, Pb <math>T_{\text{ex}} = 500^\circ\text{C}</math></b>							
Circular	37.6 / 10.1	264.9	1.60	1.95	No	147.5	No
Scalloped A	37.8 / 5.5	203.8	1.36	1.64	No	139.6	No
Scalloped B	38.2 / 2.2	160.8	1.03	1.54	No	120.6	No
<b>ELTA-CL LANL Option 2: <math>L_{\text{riser}} = 3 \text{ m}</math>, Pb <math>T_{\text{ex}} = 500^\circ\text{C}</math></b>							
Circular	37.7 / 8.2	299.9	1.30	1.60	No	147.9	No
Scalloped A	37.8 / 5.1	257.9	1.25	1.52	No	141.1	No
Scalloped B	38.2 / 2.2	219.9	1.01	1.52	No	122.5	No
<b>ELTA-CL UNM-ISNPS Option: <math>L_{\text{riser}} = 3 \text{ m}</math>, Pb <math>T_{\text{ex}} = 500^\circ\text{C}</math></b>							
Circular	37.7 / 9.9	322.5	1.57	1.92	No	159.4	No
Scalloped A	37.8 / 5.4	262.7	1.35	1.62	No	150.4	No
Scalloped B	38.3 / 2.2	220.4	1.03	1.54	No	128.7	No

## 2.2. Effect of Riser Length on Performance of GLP Option

As delineated in Fig. 5, increasing the riser length of the ELTA-LC only results in comparatively small increases in the Pb flow rate. The increase in flow rate decreases gradually with increased riser height and is best for a 3 m tall riser. Additional increases of the riser height result in a gradually smaller increases in the flow rate. Most of the increase in the average gas void fraction or decrease in the average density in the riser occurs in the last 1.5-2 m of the riser length. The high static pressure head of the molten Pb in the lower part of the riser limits the growth of the injected gas bubbles and the increase in the local average void fraction.

### 3. Improved Designs of the Annular Linear Induction Pump (ALIP)

The ALIPs are a type of electromagnetic pump that have been widely used for circulating liquid metal coolants in test loops and fast test reactors (Kelly, 2020; Polzin, 2010; Nashine, 2020). Induction from three phase alternating current (3 $\phi$ -AC) passing through the copper windings onto a ferromagnetic stator in the form of flat “pancake” coils produces a linearly traveling magnetic field. Intersection of the traveling magnetic field lines with the liquid metals in the annular duct induces electric current in the liquid metal in same plane as the magnetic field. The interaction of induced current and moving magnetic field produces a force in the perpendicular direction that causes the flow of the liquid metal.

The developed pressure head by the ALIP depends on the number of coil windings in the pump, the applied terminal voltage and the current frequency. Increasing the number of coil winding assemblies increases the generated pressure head, but also increases the length of the ALIP. While the developed pressure head increases proportional to the applied terminal voltage, it decreases with increasing current frequency. Further details on the developed ALIP design and earlier analyses results are reported in El-Genk et al. (2020). The present report provides performance results update of the ALIP designs with high temperature ceramic insulated Cu wires, and 3 insulated Cu wires per phase. It also presents the obtained results of the effect of the insulated Cu wires diameter (12 and 12 AWG) and the total length of the ALIP design with 68.8 mm diameter footprint on the performance characteristics.

The developed ALIP designs fit within the riser tube of ELTA-CL with an inner diameter of 68.8 mm and are placed near the exit of the riser above the 3-rod test bundles (El-Genk et al., 2020). Developing an ALIP design for a riser tube diameter of 57.0 mm is not practical because of the very small width of the annular flow channel (El-Genk et al., 2020).

The ceramic insulated Cu alloy wires in the developed ALIP designs which can operate at Pb exit temperature of 500°C without active cooling. At higher Pb temperatures of up to 700-750°C, the stator and Cu wires could be cooled to maintain its temperature at 500°C, by rejecting the dissipating heat directly to the VTR sodium flow. This cooling option would have to be incorporated into the ELTA-CL design.

The performed parametric analyses also investigated the effects of changing the applied voltage (120, 240, and 360 VAC, 3-phase), the voltage frequency (30, 60, and 90 Hz), the total pump length (60, 90, and 120 cm), the number of Cu coils per phase (3 and 4 wires), and the diameter of ceramic insulated Cu wire (12 and 18 AWG). The obtained results for the three design options of the ELTA-CL with the selected ALIP design with best performance are compared in Table 5.

#### *3.1. Effects of ALIP Length and Wire Diameter on Performance*

Figure 6 compares the characteristics for the improved ALIP designs of total length of 60, 90 and 120 cm, and with ceramic insulated Cu wires for high temperature operation. Details of the ALIP design and cross-sectional views are included in an earlier progress report (El-Genk et al., 2020). The best ALIP performance is that presented in Fig. 6 for three-phase, 240VAC at 30 Hz. The results in Fig. 6 shows the superior performance of the 90 cm and 120 cm long ALIPs, which deliver high pumping heads of up to more than 1100 kPa and molten Pb circulation rates up to ~ 20 kg/s. For the same Cu wire diameter (12 or 18 AWG), the pumping head increases with increased total length of the ALIP with 3 wires per phase. The larger diameter ceramic insulated Cu wires (12 AWG) increase the performance of the ALIP, but also increases the rate of heat dissipation.

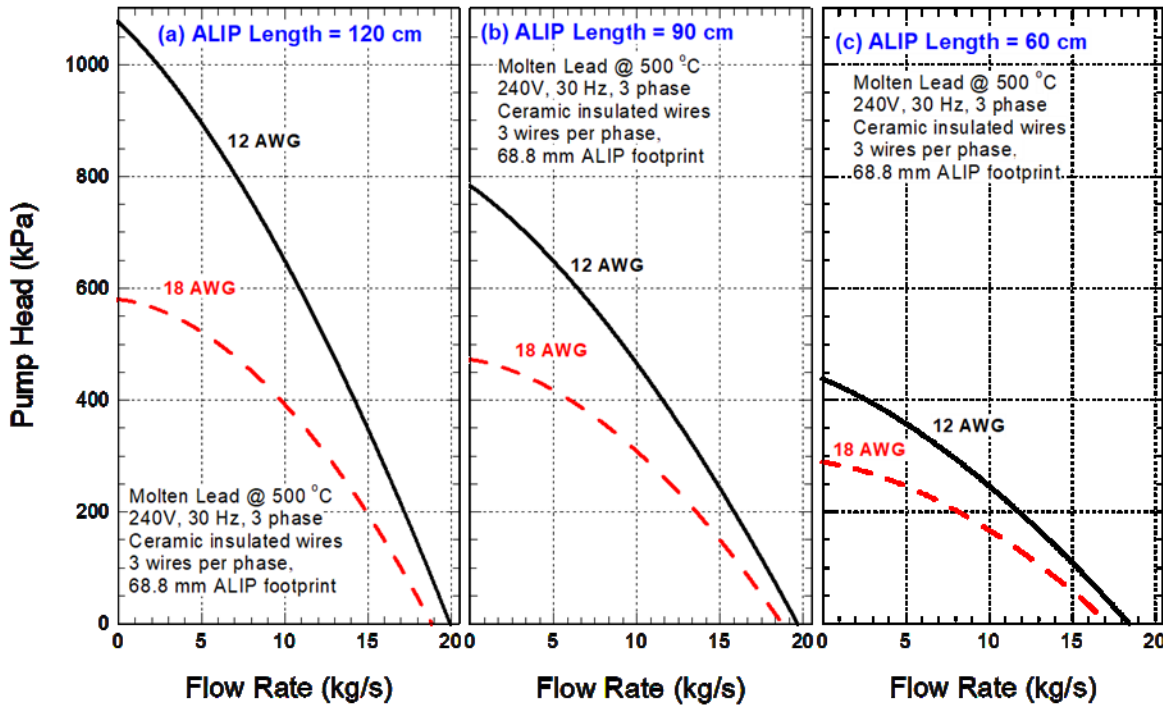


**Fig. 6:** Calculated ALIP performance characteristics at a molten lead exit temperature of 500°C.

Table 5 compares the calculated performance of the 90 cm and 120 cm long improved ALIP designs for the ELTA-CL with 18 AWG ceramic insulated Cu wires, 3 wires per, and 3-phase 240VAC at 30 Hz. The results in Table 5 are for the ALIP footprint that fits in a 68.8 mm diameter riser tube in the LANL Option 2 design and the UNM-ISNPS proposed design of the ELTA-CL (Table 2).

The high generated pumping heads of the improved 90 cm and 120 cm long ALIP designs make it possible to achieve flow velocities of molten Pb in the 3-rod test bundles (Fig. 1) which can exceed the desired value of 3 m/s (Table 1). The ALIP designs in Table 5 dissipate ~3.2 - 4.3 kW, which decrease the attainable average liner power for the test fuel rods by ~ 10%. As indicated earlier and shown in Fig. 3 and listed in Tables 4 and 5, the average linear power per test rods strongly depend on the width of the He gap in the wall between the molten Pb flow in the downcomer and the VTR primary Na coolant flow for the ELTA-CL (Fig. 3).

In summary, the fully passive, improved ALIP designs compared in Table 5 are an attractive choice that is worthy of consideration for the ELTA-CL for operating at 500°C without requiring active cooling. For operating at higher temperatures up to 750°C, the temperature of the ceramic insulated Cu wires in the stator of the ALIPs can be maintained at 500°C by rejecting the dissipated thermal power to the VTR primary sodium coolant, which could be incorporated into the design of the ELTA-CL.

**Table 5:** Comparison of the performance of the best performing ALIPs for ELTA-CL at 500°C.

Bundle Geometry	Head / Pb Flow (kPa / kg/s)	Losses (kW)	ALIP $\eta$ (%)	Compliance with ELTA-CL Requirements				
				Velocity (m/s)		Met?	Linear Power (W/cm)	Met?
				$V_{av}$	$V_{max}$			
<b>ELTA-CL LANL Option 2: 120 cm ALIP, 240 V-3 <math>\phi</math>, 30 Hz, Coils: 3 wires per phase, Pb <math>T_{ex} = 500^\circ\text{C}</math></b>								
Circular	137.1 / 16.2	3.59	5.6	2.57	3.09	N/Y	131.3	No
Scalloped A	247.6 / 13.8	3.75	8.0	3.43	4.00	Yes	129.0	No
Scalloped B	442.3 / 8.3	4.29	7.6	3.83	5.10	Yes	120.1	No
<b>ELTA-CL LANL Option 2: 90 cm ALIP, 240 V-3 <math>\phi</math>, 30 Hz, Coils: 3 wires per phase, Pb <math>T_{ex} = 500^\circ\text{C}</math></b>								
Circular	127.2 / 15.6	3.26	5.8	2.47	2.97	No	133.2	No
Scalloped A	219.7 / 13.0	3.42	7.5	3.22	3.76	Yes	130.6	No
Scalloped B	368.1 / 7.6	3.88	6.4	3.47	4.65	Yes	121.5	No
<b>ELTA-CL UNM-ISNPS Option: 120 cm ALIP, 240 V-3 <math>\phi</math>, 30 Hz, Coils: 3 wires per phase, Pb <math>T_{ex} = 500^\circ\text{C}</math></b>								
Circular	103.5 / 16.9	3.56	4.5	2.68	3.21	No/Y	142.2	No
Scalloped A	229.4 / 14.3	3.72	7.8	3.54	4.11	Yes	139.5	No
Scalloped B	439.5 / 8.4	4.28	7.7	3.88	5.15	Yes	129.3	No
<b>ELTA-CL UNM Option: 90 cm ALIP, 240 V-3 <math>\phi</math>, 30 Hz, Coils: 3 wires per phase, Pb <math>T_{ex} = 500^\circ\text{C}</math></b>								
Circular	97.4 / 16.4	3.22	4.5	2.59	3.11	No/Y	144.2	No
Scalloped A	205.0 / 13.4	3.39	7.3	3.33	3.88	Yes	141.1	No
Scalloped B	366.0 / 7.6	3.87	6.4	3.51	4.71	Yes	130.5	No

#### 4. Improved Design of Direct Current-Electromagnetic Pump (DC-EMP)

The DC-EMP is an electromagnetic pump where the magnetic field is supplied by two permanent magnets located on either side of a rectangular flow duct. High DC electrical current to the pump flows in a perpendicular direction to but in the same plane as the magnetic field. The electrical current through the molten Pb flow duct is provided through Cu bus bar electrodes mounted to the sides of the duct wall. The interaction of the supplied current with the magnetic field generated by the permanent magnets produces an electromotive force in the perpendicular direction to the current-magnetic field plane that causes the flow of the liquid metal.

The improved design of the DC-EMP developed by UNM-ISNPS this quarter (June - September 2020) is shown in Fig. 7. The DC-EMP design has two active pumping regions, one each at the opposed poles of two parallel permanent magnets. The active sections for the flow have a rectangular channel for molten lead, which is (a x b) in cross section and c long. The DC-EMP employs ALNICO 5 permanent magnets with a curie point of  $\sim 800^{\circ}\text{C}$ . At a Pb exit temperature of  $500^{\circ}\text{C}$  the DC-EMP does not need active cooling. At higher Pb temperatures of up to  $700\text{-}750^{\circ}\text{C}$ , the magnet could be cooled to maintain its temperature at  $500^{\circ}\text{C}$ , by dissipated heat directly to the VTR sodium flow. The DC-EMP designs are passive with no moving parts and only 40 cm long plus 5 cm long inlet nozzle (Fig. 7). They are to be mounted within the riser pipe of the ELTA-CL above the 3-rod bundle test section (El-Genk et al., 2020).

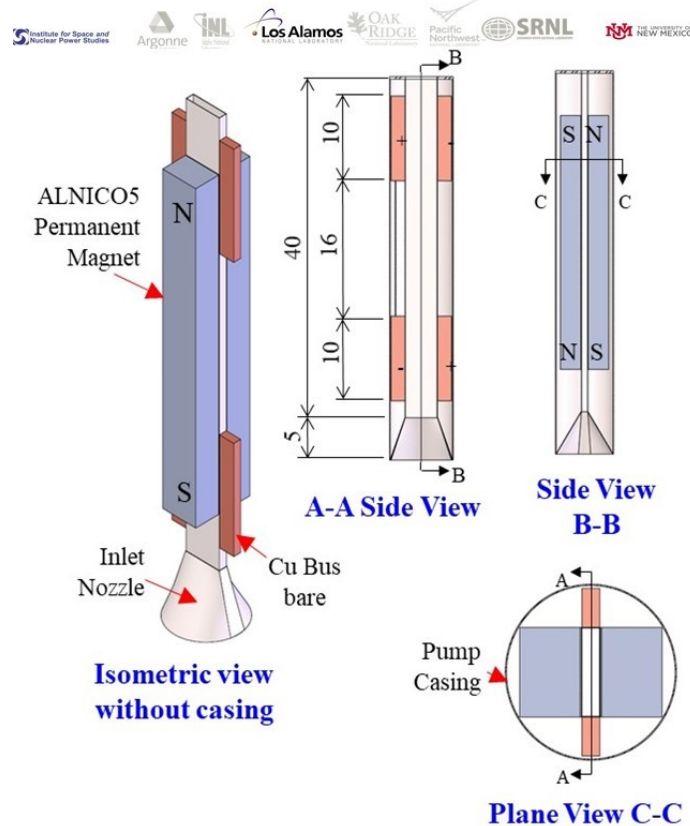


**Fig. 7:** Improved DC-EMP Design for ELTA-CL with riser tube diameters of 57.0 and 68.8 mm.

This effort investigated the effect of changing the duct dimensions, the magnet thickness, and the position of the Cu bus bars on the performance of the improved design of the miniature, submerged DC-EMP for operating at  $500^{\circ}\text{C}$  in the ELTA-CL. The results of these parametric

analyses are used to determine the optimal flow duct dimensions for enhancing the performance characteristics of the improved DC-EMP designs for riser tube inner diameters of 57.0 mm and 68.8 mm. The developed DC-EMP operation model based on the equivalent circuit approach is developed and implemented into Simulink/Matlab platform. The model is used to calculate the pump performance characteristics as functions of the Pb flow rate. The IEEE FEMM magnetic field analysis software (Meeker, 2019) is used to model the magnetic field lines for the developed DC-EMP designs with ALINCO 5 magnets and to determine the effective magnetic field strength for the DC EMP performance model.

#### 4.1. DC-EMP Performance Characteristics

Figure 8 compares the calculated performance characteristics for the improved optimized DC-EMP designs for ELTA-CL with riser tube inner diameters of 57.0 mm and 68.8 mm. The larger diameter DC-EMP produces 29-52% higher pumping head compared to that of the DC-EMP for the smaller 57.0 mm riser tube diameter. The produced pressure heads by the improved DC-EMP designs is much lower than what those achievable using the improved ALIP designs, discussed in the previous section.

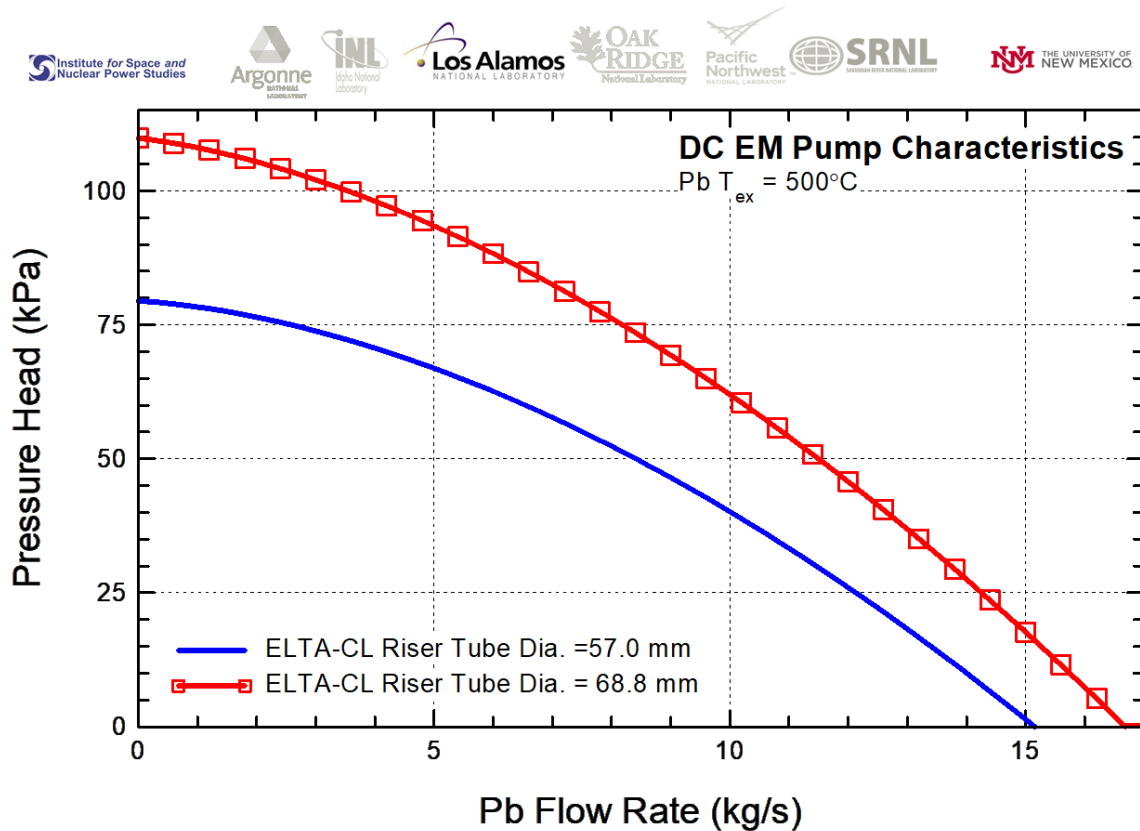


**Fig. 8:** Calculated DC-EMP performance characteristics at a molten lead temperature of 500°C.

Table 6 summarizes the performance of the improved designs of the DC-EMP for the ELTA-CL design options in Table 2. The supplied current to the DC-EMP range from 1130 -1055 A at a terminal voltage of ~1.0 VDC. The dissipated thermal power by the DC-EMP designs of ~1.0 kW is much lower than that generated by the ALIP. With the improved DC-EMP designs it is possible to achieve an average flow velocity of up to 1.96 m/s and a maximum velocity of up to 2.47 m/s of molten lead in three different geometries investigated for 3-rod test bundles (Fig. 1).

**Table 6:** Performance comparisons of the developed improved DC-EMPs for the three designs of the ELTA-CL in Table 2 at molten Pb temperature of 500°C.

Test Article Geometry	Head / Pb Flow (kPa / kg/s)	Losses (kW)	Pump $\eta$ (%)	Compliance with ELTA-CL Requirements				
				Velocity (m/s)		Met?	Linear Power (W/cm)	Met?
				$V_{av}$	$V_{max}$			
<b>ELTA-CL LANL Option 1: a = 29.84 mm, b = 8.2 mm, c = 100 mm, I = 1130 A, 0.98 VDC, Magnetic Flux Density = 3140 G, Pb <math>T_{ex}</math> = 500°C</b>								
Circular	38.9 / 10.2	1.07	3.4	1.61	1.96	No	141.3	No
Scalloped A	58.3 / 6.9	1.06	3.5	1.71	2.04	No	136.2	No
Scalloped B	73.2 / 3.2	1.08	2.0	1.47	2.13	No	121.2	No
<b>ELTA-CL LANL Option 2: a = 34.5 mm, b = 7.2 mm, c = 100 mm, I = 1055 A, Terminal Voltage = 1.00 VDC, Magnetic Flux Density = 4149 G, Pb <math>T_{ex}</math> = 500°C</b>								
Circular	59.3 / 10.3	1.00	5.6	1.64	1.99	No	144.5	No
Scalloped A	79.4 / 7.5	1.00	5.4	1.86	2.22	No	140.6	No
Scalloped B	99.3 / 3.7	1.02	3.3	1.70	2.43	No	127.7	No
<b>ELTA-CL UNM Option: a = 34.5 mm, b = 7.2 mm, c = 100 mm, I = 1055 A, Terminal Voltage = 1.00 VDC, Magnetic Flux Density = 4149 G, Pb <math>T_{ex}</math> = 500°C</b>								
Circular	50.1 / 11.5	1.00	5.2	1.82	2.21	No	155.3	No
Scalloped A	76.7 / 7.9	1.00	5.5	1.96	2.33	No	150.2	No
Scalloped B	99.1 / 3.8	1.02	3.4	1.72	2.47	No	135.1	No

## 5. Improved Design of Axial Centrifugal Flow Mechanical Pump (MP)

During the last quarter (June-September 2020) we have improved the performance of previously reported miniature axial centrifugal flow mechanical pump design (El-Genk et al., 2020) for the ELTA-CL. The innovative impeller MP design for riser diameters of 57.0 mm and 68.8 is quite effective. The MP impeller mounts at top of ELTA-CL riser tube with a fitted shroud, thus does not occupy much space in the riser tube. The molten Pb flow enters the pump axially to the impeller and then exits radially, with aid of curved flow guide, into the annular downcomer of the ELTA-CL. Several short and radially arranged guide vanes are used at the top of the downcomer effectively dampens the swirling flow exiting MP impeller blades and insure a smooth downwards flow of molten Pb in the ELTA-CL downcomer.

The improvements to the MP design this quarter include smoothing the tips of the impeller blades and the inside surface of the entrance shroud wall. They reduced the frequency and intensity of the induced turbulent vortices in the flow exiting the impeller plates, decreased the pressure losses through the impeller and increased the pump performance characteristics. In addition, a consistent methodology is developed to ensure that the state variables for the pump in the CFD analyses are fully converged. These variables include the pressure head, the molten Pb flow rate and the torque for the impeller shaft. It took days and some time a couple of weeks for a full conversion to be realized for each data point of the pressure head-flow rate on the MP characteristics.

Further details of the MP design optimization process and images of 3-D printed plastic impeller are included in an earlier progress report (El-Genk et al. 2020). Operating the developed MP miniature impeller would require employing either a long drive shaft connection to a motor outside the reactor vessel, or shorter shaft powered by a local gas turbine. The implemented CFD modeling methodology for the optimized MP design used the STAR-CCM+ commercial software (Siemens PLM, 2019), which is successfully validated using reported experimental data for a Russian Pb axial flow pump design (Beznosov et al. 2017). The calculated MP pressure head was in good agreement with the reported experimental data to within 10%.

The developed design optimization methodology of the MP includes performing 3D-CFD analyses of the flow field to and in between the impeller blades to calculate the pump characteristics as a function of the rotation speed of the impeller shaft. This methodology, detailed elsewhere (El-Genk et al. 2020), was used to optimize the pump characteristics for either maximizing the pumping power, the pump efficiency, of the pump pressure head. The results of optimizing the pumping power consistently gave the best pump characteristics, and thus used in the present results. Accomplished work on the design optimization of the MP also included developing two improved designs for ELTA-CL with riser tube diameters of 57.0 mm and 68.8 mm, and performing CFD analyses for rotation speeds of the impeller shaft of 1,500, 2,000, 2,500 and 3,000 rpm. The calculated velocity and pressure flow field for the circulated molten Pb at 500°C for the different shaft rotation speeds and footprint diameter of the MP are analyzed and compared.

### 5.1 MP Performance Results

The results of the performance analyses of the MP optimized impeller designs for maximizing the pumping power are used to develop the pump designs for the ELTA-CL with 57.0 mm and 68.8 mm riser tube diameters. We have successfully demonstrated using 3D printing to manufacture a MP impeller for future testing in the water loop currently under construction at LANL.

Fig. 9 compares the calculated performance characteristics curves for the optimized MP designs for 57.0 mm and 68.8 mm riser tube diameters for impeller shaft rotation speeds of 1,500 and 2,500 rpm. The characteristic curves for the MP are much flatter than those of the ALIP or DC-EMP. Increasing the impeller diameter from 57.0 mm to 68.8 mm significantly increases the generated pumping head by 65-90%. The larger diameter impeller produces a pressure head more than 400 kPa at a shaft rotation speed of 2,500 rpm.

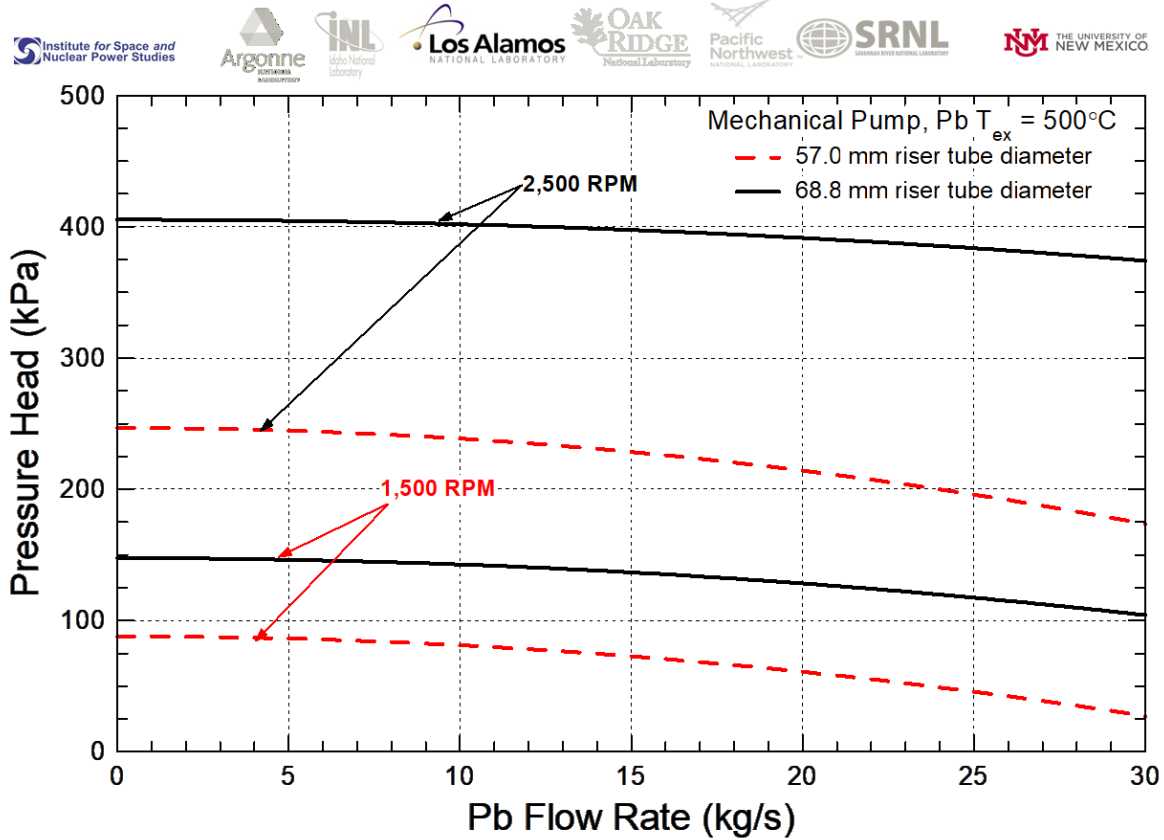


**Fig. 9:** MP performance characteristics at a molten lead exit temperature of 500°C.

Table 7 summarizes the performance parameters of the optimized MP designs for ELTA-CL at Pb exit temperature of 500°C. At a shaft rotational speed of 2,500 rpm, the optimized MP with 68.8 mm diameter impeller is capable of meeting or exceeding the desired 3 m/s average Pb velocity in the 3-rod test bundles of different geometries (Fig. 1). The heat dissipation by the MP designs of 0.12-1.3 kW is much lower than that for the ALIP but comparable to those for the DC-EMP, it increases with increasing the rotational speed of the impeller shaft (Table 7). The efficiency of the MP of as much as 48.8%, is much higher than those calculated for the DC-EMP and ALIP (Tables 5. 6).

**Table 7:** Comparison of the performance parameters of the optimized MP designs for ELTA-CL at Pb temperature of 500°C.

Bundle Geometry	Head / Pb Flow (kPa / kg/s)	Losses (W)	Pump $\eta$ (%)	Compliance with ELTA-CL Requirements				
				Velocity (m/s)		Met?	Linear Power (W/cm)	Met?
				$V_{av}$	$V_{max}$			
<b>ELTA-CL LANL Option 1: 1,500 RPM, Pb <math>T_{ex} = 500^\circ\text{C}</math></b>								
Circular	72.4 / 14.2	0.12	44.4	2.25	2.71	No	151.0	No
Scalloped A	82.6 / 8.3	0.08	46.1	2.06	2.45	No	145.4	No
Scalloped B	88.5 / 3.6	0.06	31.2	1.63	2.34	No	130.4	No
<b>ELTA-CL LANL Option 1: 2,500 RPM, Pb <math>T_{ex} = 500^\circ\text{C}</math></b>								
Circular	199.1 / 24.4	0.58	44.5	3.87	4.58	Yes	152.1	No
Scalloped A	231.2 / 14.5	0.36	46.8	3.59	4.17	Yes	149.6	No
Scalloped B	243.7 / 6.2	0.25	36.3	2.83	3.86	No/Y	139.8	No
<b>ELTA-CL LANL Option 2: 2,500 RPM, Pb <math>T_{ex} = 500^\circ\text{C}</math></b>								
Circular	378.0 / 28.0	1.07	48.4	4.44	5.23	Yes	151.6	No
Scalloped A	394.4 / 17.8	0.73	47.9	4.41	5.09	Yes	151.1	No
Scalloped B	403.2 / 7.9	0.74	29.0	3.65	4.87	Yes	143.1	No
<b>ELTA-CL UNM Option: 2,500 RPM, Pb <math>T_{ex} = 500^\circ\text{C}</math></b>								
Circular	367.2 / 33.1	1.30	48.7	5.25	6.16	Yes	162.2	No
Scalloped A	392.8 / 19.0	0.76	48.8	4.72	5.43	Yes	162.0	No
Scalloped B	403.1 / 8.1	0.74	29.5	3.70	4.94	Yes	152.2	No

## 6. Summary and Findings

The UNM-ISNPS has developed optimized designs and conducted performance analyses of miniature pumping options for three different potential designs of the ELTA-CL at 500°C Pb exit temperature. The investigated pumping options include the Gas Lift Pumping (GLP), Annular Linear Induction Pump (ALIP), Direct Current-Electromagnetic Pump (DC-EMP), and axial-centrifugal flow Mechanical Pump (MP). A comparison summary of the performance parameters of these four pumping options is provided in Table 8. The reported analyses results include the pump performance characteristics, and when applicable, power supply requirement, efficiency, power consumption, thermal power dissipation, and CFD flow fields characterization and estimates of the average linear power of the test fuel rods.

**Table 8:** Comparison summary of the performance of the four pumping options investigated for the ELTA-CL at molten Pb exit temperature of 500°C.

Parameter	GLP	ALIP	DC-EMP	MP	Notes
<b>Operation</b>	Passive <sup>+</sup>	Passive	Passive	Active*	*Argon injection 160-320 mg/s
<b>Head (kPa)</b>	37 - 38	97 - 442	39 - 99	72 - 403	*Impeller rotation up to 2,500 rpm
<b>Molten Pb Flow Rate (kg/s)<sup>#</sup></b>	2.2 - 10.1	7.6 - 16.9	3.2 - 11.5	3.6 - 33.1	#Depends on 3-rod bundle geometry
<b>Power Supply (kW)<sup>#</sup></b>	None <sup>@</sup>	3.44 - 4.64	1.05 - 1.10	0.18 - 2.88 <sup>\$</sup>	@External pressurized Argon gas supply
<b>Losses (kW)<sup>#</sup></b>	None	3.2 - 4.3	~ 1.0	0.1 - 1.3	\$Shaft Power
<b>Efficiency (%)<sup>#</sup></b>	N/A	4.5 - 7.8	2.0 - 5.6	29.0 - 48.8	
<b>Flow Velocities:</b>					
<b>V<sub>av</sub> (m/s)</b>	1.01 - 1.60	2.47 - 3.88	1.47 - 1.96	1.63 - 5.25	
<b>V<sub>max</sub> (m/s)</b>	1.52 - 1.95	2.97 - 5.15	1.96 - 2.47	2.34 - 6.16	

Result show that the test the 3-rod bundle geometry and the pumping option insignificantly affect the fuel rod average linear power, except with ALIP is ~10% lower due to the higher heat dissipation rate. The rod linear power is mostly constrained by the heat rejection rate for the flowing molten PB in the downcomer of the ELTA-CL to the VTR primary Na coolant. This heat rejection rate strongly depends on the width of the He filled gap in the wall separating the Pb annular downcomer from the up flow of the VTR Na coolant. It increases with decreased He gap width and/or increased lead exit temperature. With a He gas gap width of 0.5 mm and 500°C Pb exit temperature, the average linear power of the test fuel rods would be within the desirable requirements of 240 – 400 W/cm. For higher Pb temperature of 700°C, He gas gap width that is as large as 1.5 mm would meet the average linear power requirements for the test fuel rods.

The GLP option, the simplest with no thermal power dissipation, is only capable of achieving comparatively low Pb flow rates. The flow velocities in the 3-rod test bundles in ELTA-CL with a riser height of 3.0 m are below the desired 3 m/s average velocity (*max. attainable* ~ 1.6 m/s in *circular bundle geometry*). Increasing the riser tube diameter insignificantly affects the GLP performance but does increase the required Ar injection rate for the same Pb flow rate. Note that

best performance results are when the average void fraction of molten Pb-gas mixture in the ELTA-CL riser tube is kept  $\leq 0.20$ . For this exit void fraction, results of parametric investigation of ELTA-CL performance with GLP determined that the flow rate increases with increased riser height up to 3.0 m, then very little beyond.

The ALIP is also passive with no moving parts. The developed ALIP design fits within a riser tube that is 68.8 mm, but not a 57.0 mm in diameter. The ALIP designs for best performance are those with total length of 90 or 120 cm, 240 VAC-3- $\phi$ , 30 Hz terminal voltage and 3 ceramic insulated Cu wires (12 AWG) per phase. The commercially available ceramic insulated 12 and 18 AWG Cu wire coils, require no cooling when operating at a Pb exit temperature of 500°C. The developed ALIP design is capable of supplying the highest pumping head of all four pumping options investigated and can meet or exceed the 3 m/s flow velocity requirements in the ELTA-CL 3-rod test bundles. This pump also dissipates the highest thermal power (3.2-4.3 kW), which decreases the average linear power of the test fuel rods by  $< 10\%$ .

The DC-EMP is passive with no moving parts and requires high-current and very low voltage power supply. The developed DC-ALIP designs employ ALNICO 5 permanent magnets, which do not require external cooling at 500°C. The two DC-EMP designs are developed to fit within riser tube diameters of 57.0 and 68.8 mm. The DC-EMP for the 68.8 mm riser tube diameter increases the pumping head by 29-52% over that for the 57.0 mm riser tube diameter. Both pump designs dissipates  $\sim 1$  kW of thermal power. The developed DC-EMP designs are short of meet the flow velocity requirements in ELTA-CL of 3 m/s (*max. attainable is  $\sim 1.96$  m/s in at 500°C*)

Improved designs of the innovative axial-centrifugal flow MP are developed for ELTA-CL designs with riser tube diameters of 57.0 mm and 68.8 mm. The best and consistent performance results are obtained for the optimized MP designs for maximum pumping power. The pumping characteristics increase with increased rotation speed of impeller shaft (1,500, 2,500, and 3,000 rpm). At the same impeller rotation speed, the MP designs for a riser tube diameter of 68.8 mm produces 65-90% higher pressure head compared to that of the MP design for the smaller riser tube diameter of 57.0 mm. The dissipation power by the MP is relatively low, ranging from  $\sim 0.1$ -1.3 kW, depending on the molten Pb rate and the impeller shaft speed. Results show that the developed MP designs are capable of matching or exceeding the desirable requirement of 3 m/s flow velocity of molten Pb in the 3-rod test bundles. Additionally, the calculated molten Pb velocities at the tips of impeller blades are within acceptable range for corrosion and erosion concerns ( $< 20$  m/s for pump shaft rotation speeds of  $\leq 2500$  RPM).

## References

- Beznosov, A.V., Lvov, A.V., Bokov, P.A., Bokov, T.A., Razin, V.A., Experimental studies into the dependences of the axial lead coolant pump performance on the impeller cascade parameters, Nuclear Energy and Technology, 3(2), 2017, 141-144
- El-Genk, M.S, Schriener, T., Hahn, A., Altamimi, R., Design Optimization and Performance of Pumping Options for VTR Extended Length Test Assembly for Lead Coolant (ELTA-CL), Technical Report Number: UNM-ISNPS-4-2020, Albuquerque, NM, USA June 2020.
- Kelly, B., Idaho National Laboratory, personal communication, January 2020
- Meeker, D.C., 2020, Finite Element Method Magnetics, <http://www.femm.info>
- Nashine, 2020, “Design, development and testing of a sodium submersible Annular Linear Induction Pump for application in sodium cooled fast reactor,” Annals of Nuclear Energy, 145, 107494
- Nishi et al., “Experimental study on gas lift pump performance in lead-bismuth eutectic,” Proc. 2003 Int. Congress on Advanced Nuclear Power Plant, ICAPP’03, Cordoba, Spain, May 2003.
- Polzin, K.A., et al., 2010, Performance testing of a prototype annular linear induction pump for fission surface power, NASA report NASA/TP-2010-216430, Marshall Space Flight Center, Huntsville, Al.
- Siemens PLM, 2019, STAR-CCM+ Release 13.06, <http://www.cd-adapco.com/>
- Shi et al., “Experimental investigation of gas lift pump in a lead-bismuth eutectic loop, Nuclear Engineering and Design, 320, 2018, 516-523.